Identification of Neighboring Atoms in Extended X-ray Absorption Fine Structure

Folim G. Halaka, John J. Boland, and John D. Baldeschwieler*

Contribution from the Division of Chemistry and Chemical Engineering, California Institute of Technology, Pasadena, California 91125. *Received September 28, 1983*

Abstract: A method for the identification of neighboring atoms in extended X-ray absorption fine structure (EXAFS) spectroscopy is presented. This method takes advantage of the differences in scattering phases between elements. The total phase from the first shell of atoms is isolated and compared with that for compounds with the same absorber but different scatterers. To obtain an accurate isolation of the total phase, a new method of isolating peaks in distance (r) space is introduced. This method consists of truncating the peak in a region above the side lobes and translating it down to the distance axis. The modulus of the Fourier transform (FT) of each point in r space is reduced, but the phase is constrained to be the same as that in the original data. The total phase isolated by this method is then fitted to an equation of the form $c_0 + c_1k + c_2k^2$, where k is the photoelectron wavenumber. The constant coefficient (c_0) in the fit is shown to be a quantitative means of identifying the scattering atoms. To demonstrate this atom-identification scheme, the compounds $Co(acac)_3$, $[Co(en)_3]Cl_3$, and $K_3[Co(CN)_6]$ were studied (acac, acetylactone; en, ethylenediamine). The phase intercepts (c_0 coefficients) were determined from the isolated first shell of each compound and agree well with the theoretical calculations. An additional nitrogen compound, $[Co(NH_3)_6]Cl_3$, was studied, and its phase intercept was found to be virtually identical with that of $[Co(en)_3]Cl_3$. It is suggested that by comparing the phase intercept of an unknown compound with those of a series of model compounds the scattering atom in the unknown may be identified. The possibility of determining the composition of shells containing different atoms is also discussed.

Extended X-ray absorption fine structure (EXAFS) spectroscopy, the modulation of the X-ray absorption coefficient at energies above the absorption edge, has been applied to a wide range of structural problems in recent years. The use of the method is not limited by the physical state of the sample, and hence it is a valuable tool in identifying the local environments of absorbing atoms for which conventional X-ray diffraction methods are not applicable, for example, in certain metalloproteins,[1-3] solutions,[4,6] and gases.[7]

The single scattering EXAFS expression may be written as[8]

$$\chi(k) = -(1/k)\sum_j A_j \sin [2kr_j + \delta'_j(k)] \quad (1)$$

where A_j is the amplitude function. A_j contains the number of atoms of type j, the Debye-Waller factor, and the inelastic loss term. k is the photoelectron wavenumber defined by

$$k = [2m(\hbar\omega - E_0)]^{1/2}/\hbar \quad (2)$$

where ω is the frequency of the X-rays and E_0 is the threshold energy. $\delta'_j(k)$ is the composite phase function,

$$\delta'_j(k) = \delta_a(k) + \delta_j(k) \quad (3)$$

$\delta_a(k)$ is the phase change in the photoelectron wave due to the absorbing atom potential, and $\delta_j(k)$ is the phase of the scattering amplitude associated with atom j.

Model compounds are used extensively in EXAFS to determine atom types as well as bond distances. Chemical intuition and information available from other techniques usually reduce the number of model compounds that are required. There is, however, usually no independent method to identify the scattering atoms. The backscattering amplitude may exhibit Ramsauer-Townsend-type resonances and may be used to identify scattering atoms.[9] These resonances, however, are experimentally observable for heavy scattering atoms only. The identification of light atoms is more difficult since their backscattering amplitudes are small and do not exhibit such structure. A method for distinguishing light atoms (as scatterers) would thus be a valuable addition to EXAFS. For example, differentiating carbon, nitrogen, or oxygen in metalloproteins or in surface chemistry would be of great value in structural determination.

In this paper, we present a method for identifying scattering atoms by comparing their phases with those of known compounds. We exploit the information contained in the nonlinear phases through least-squares curve fitting to show the distinguishability of carbon, nitrogen, and oxygen in a series of cobalt complexes. Theoretical calculations of scattering phases by Teo and Lee[10] clearly demonstrate this possibility. We now show this identification is possible from phases properly extracted from EXAFS data. We also introduce a new approach for isolating peaks in r space and for back transformation into k space which minimizes distortion of the phase.

Basis for the Atom-Identification Scheme

The total phase of a absorber-scatterer pair in an unknown compound is given by

$$\phi_{aj}{}^u = 2kr_j{}^u + \delta_a(k) + \delta_j{}^u(k) \quad (4)$$

where the superscript u denotes an unknown and the subscripts a and j denote an absorbing and scattering atom, respectively. The absorbing atom can easily be identified by its absorption edge and is assumed to be known. For a known (model) compound with the same absorber,

$$\phi_{aj} = 2kr_j + \delta_a(k) + \delta_j(k) \quad (5)$$

we will assume that $\delta_a(k)$ and $\delta_j(k)$ can be expressed as polynomials in k.

$$\delta_a(k) = a_0 + a_1k + a_2k^2 + \ldots$$

$$\delta_j(k) = b_0 + b_1k + b_2k^2 + \ldots \quad (6)$$

Substituting $\delta_a(k)$ and $\delta_j(k)$ into eq 5 yields

$$\phi_{aj} = (a_0 + b_0) + (2r_j + a_1 + b_1)k + (a_2 + b_2)k^2 + \ldots \quad (7)$$

or

$$\phi_{aj} = c_0 + c_1k + c_2k^2 + \ldots$$

similarly for an unknown compound

$$\phi_{aj}{}^u = c_0{}^u + c_1{}^uk + c_2{}^uk^2 + \ldots \quad (8)$$

(1) Eisenberger, P.; Okamura, M. Y.; Feher, G. *Biophys. J.* **1982**, *37*, 523.
(2) Chance, B.; Fischett, R.; Powers, L. *Biochemistry* **1983**, *22*, 3820.
(3) Powers, L. *Biochim. Biophys. Acta* **1982**, *683*, 1.
(4) Hayes, T. M.; Alen, J. W.; Tauc, J.; Giessen, B. C.; Hauser, J. J. *Phys. Rev. Lett.* **1975**, *40*, 1282.
(5) Eisenberger, P.; Kincaid, B. M. *Chem. Phys. Lett.* **1975**, *36*, 134.
(6) Sandstrom, D. R. *J. Chem. Phys.* **1979**, *71*, 2381.
(7) Kincaid, B. M.; Eisenberger, P. *Phys. Rev. Lett.* **1975**, *34*, 1361.
(8) Sayers, D. E.; Lytle, F. W.; Stern, E. A. *Adv. X-Ray Anal. B: Condens. Matter* **1970**, *13*, 248.
(9) Lee, P. A.; Beni, G. *Phys. Rev.* **1977**, *B15*, 2862.
(10) Teo, B. K.; Lee, P. A. *J. Am. Chem. Soc.* **1979**, *101*, 2815.

0002-7863/84/1506-5408$01.50/0

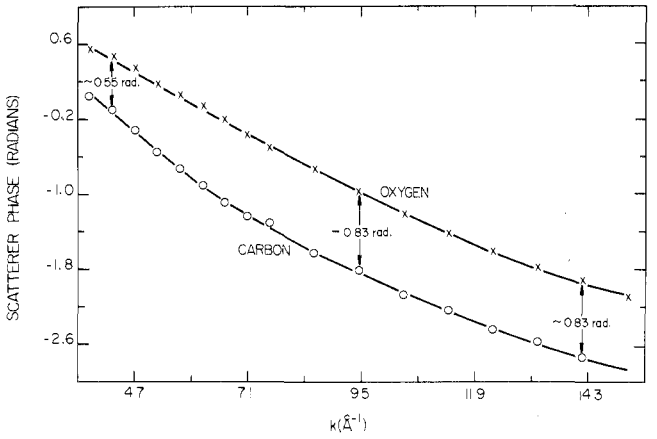

Figure 1. Scattering phases of carbon (○) and oxygen (×) as calculated by Teo and Lee.[10] The solid curves are spline fits to the calculated data.

If the scatterers are the same in both unknown and model compounds, the corresponding coefficient in eq 7 and 8 will be the same provided that the phase isolation is done adequately. In general, the phase difference between neighboring atoms in the periodic table is a smooth function of atomic number, the larger the atomic number the more positive the phase. This monotonic behavior is especially true at high k values.[10] Therefore the scattering phase of, for example, oxygen is larger at all practical k values than that of carbon.

The method employed in this work exploits the difference in scattering phase between atoms as a means for their identification. To illustrate this last point we show in Figure 1 the calculated scatterer phase functions of Teo and Lee[10] for carbon and oxygen. Note that the curves converge slightly at lower k values. It is apparent that the region of maximum phase separation and hence the best range for our calculation is from $k \sim 6$ to 13 Å^{-1}. It is also apparent that a least-squares fitting method should give c_0 terms that are well separated for carbon and oxygen since their scatterer phases are slowly varying. This is the basis for the present work. The value of the c_0 coefficient of an unknown compound may be compared to that of a series of model compounds. In this manner the nature of the scattering atom may be established. Note that since c_0 is the phase intercept at $k = 0$ Å^{-1} this atom-identification scheme is insensitive to the absorber–scatterer distance.

Data Acquistion and Analysis

All EXAFS measurements were made at room temperature and in the transmission mode with use of the Caltech laboratory EXAFS spectrometer (to be described elsewhere). The cobalt in the cobalt complexes used in the present study is in the +3 formal oxidation state. All compounds were analytical grade reagents. EXAFS samples were prepared by dissolving a known weight of material in a solvent to make a saturated solution. Another solvent (in which the compound is sparingly soluble) is then added to precipitate the compound in fine powder form. The powder was filtered, dried, and stored on a polycarbonate membrane. The thickness of the samples was calculated to absorb 70% of the X-ray beam 100 eV above the absorption edge. This method of preparing the sample was found superior, for example, to grinding the sample material to obtain a uniform particle size.

In transmission experiments, the total absorption coefficient, $\mu(k)$ is measured as

$$\mu(k)x = \ln (I_0/I) \tag{9}$$

where x is the sample thickness, I_0 is the incident X-ray beam intensity, and I is the intensity after the beam passes through the sample. $\chi(k)$ in eq. 1 is then calculated as

$$\chi(k) = \frac{\mu_c(k) - \mu_0(k)}{\mu_0(k)} \tag{10}$$

where $\mu_c(k)$ is the absorption coefficient corrected for absorption by electrons other than those of the edge under study. This correction is done by using the Victoreen formula

$$\mu_c(k) = \mu(k) - \mu_v(k) \tag{11}$$

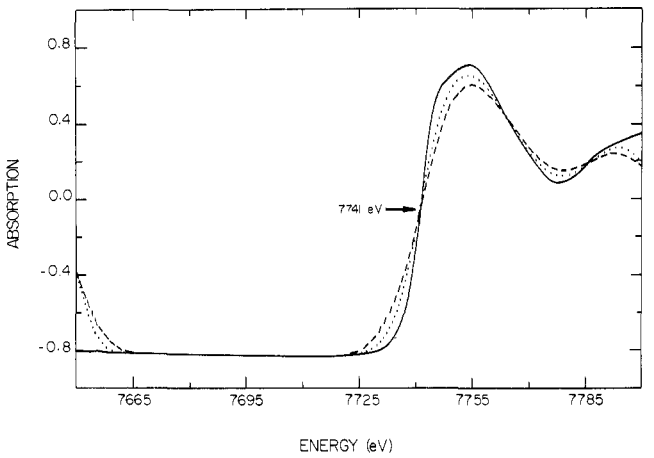

Figure 2. Determination of the threshold energy (E_0) for Co(acac)$_3$. The solid line is the original data. The dotted and dashed curves correspond to convoluting the data with Gaussian functions of full width at half-maximum (fwhm) of 16 and 32 eV, respectively. The unique intersection point at the edge corresponds to the E_0 used in this work.

$\mu_v = a\lambda^3 - b\lambda^4$ where a and b are constants and λ is the wavelength of the X-ray photon. $\mu_0(k)$ is the background absorption of the absorbing atom in the absence of ligands for the same sample thickness.

There are several problems that have to be overcome before a successful interpretation of the EXAFS data is possible. It is apparent from eq 1 and 10 that a knowledge of μ_0 is essential before a comparison of the theoretical expression with the experimental data may be attempted. It is also evident from the definition of k (eq 2) that an accurate estimate of E_0 is necessary for a correct k scaling. An accurate k scaling is important since the data are typically Fourier transformed to give peaks in r space; the position of these peaks will depend on the choice of E_0. An incorrect k scale will also hamper attempts to least-squares fit the theoretical expression (eq 1) to the data. The presence of nonlinear phase shifts also complicates the data analysis since this results in a distribution of frequencies in k space. The transformed peaks in r space are thus broad and asymmetric. This nonlinearity will also affect the peak positions in r space if different k ranges are taken for transformation. For this reason, data analyses of model compounds and unknowns are typically Fourier transformed with the same k range.

In an earlier communication,[11] we presented a method for the determination of both μ_0 and E_0. In that method, the raw EXAFS spectrum is convoluted with a series of Gaussian functions resulting in a damped EXAFS. The intersection points of this series of transformed spectra are used to generate the background absorption. We have also demonstrated that a unique intersection point of such a series of spectra exists at the absorption edge and that this intersection point provides a good measure of the threshold energy. An example of such an intersection point is shown in Figure 2 for Co(acac)$_3$. The distortions that occur at the edges of the data arise from the nature of the convolution algorithm.[11] The convolution method represents a straightforward approach for the determination of both μ_0 and E_0 and is the method used throughout this present work.

The atom-identification scheme requires the measurement of the phase intercept to an accuracy of at least 0.1 rad (see Figure 1). The method for isolating the data range to be transformed should minimize spurious side lobes in the Fourier transform and keep the phase unchanged. In the forward transform (FT of EXAFS data from k to r space) this may be accomplished by ensuring that the data begin and end at a node. For the back transform, however, the problem is more difficult because of the presence of side lobes about the base of the peak which is to be isolated. In this case, only the undistorted part of the peak (shaded area in Figure 4a–c) is transformed. To avoid distortions resulting from applying a window for the isolation, the desired region of the peak is translated down to the distance axis. The rest of the data in r space is set equal to zero. The peak now starts and ends at zero modulus values (nodes in both real and imaginary parts). In practice, this is accomplished by subtracting the lowest modulus value in the region to be back transformed from the modulus at every point in that region. This can be accomplished without changing the phase. If we denote the lowest modulus value by A_0, then we require that for each point

$$A_j = A_i - A_0 \tag{12}$$

(11) Boland, J. J.; Halaka, F. G.; Baldechwieler, J. D. *Phys. Rev. B: Condens. Matter B28*, **1983**, 2921.

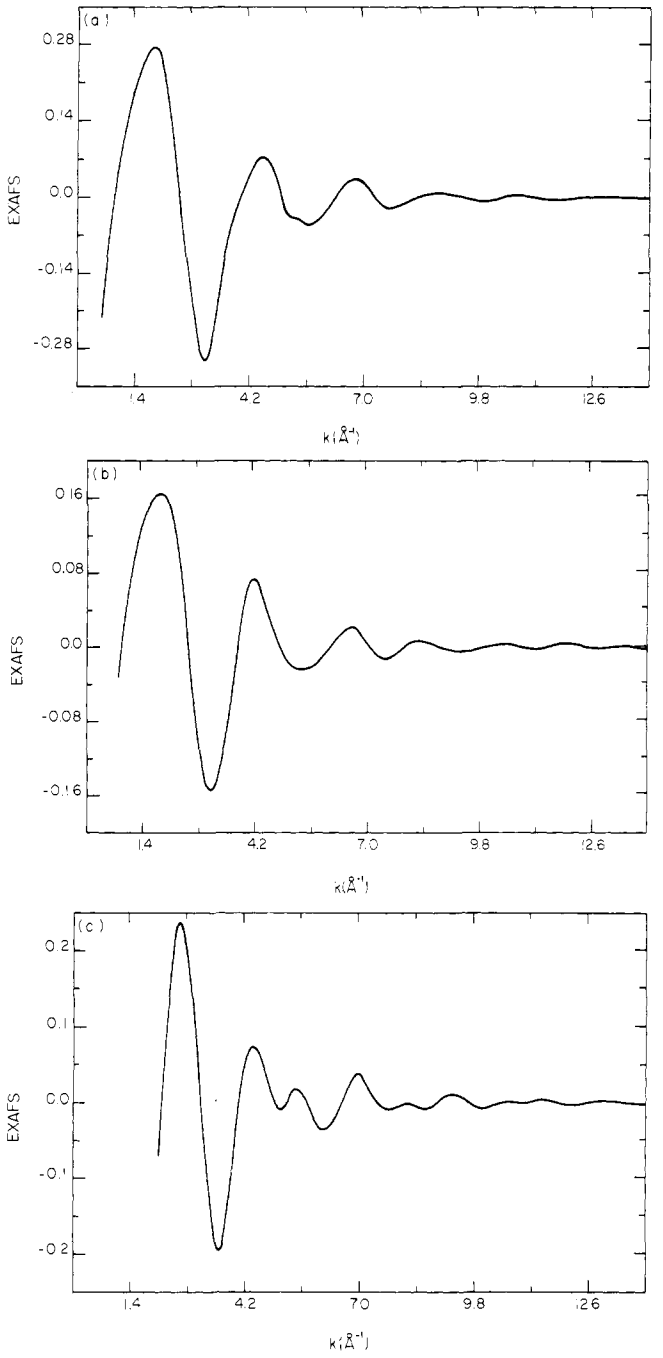

Figure 3. Isolated EXAFS spectra: (a) $Co(acac)_3$, (b) $[Co(en)_3]Cl_3$ (c) $K_3[Co(CN)_6]$.

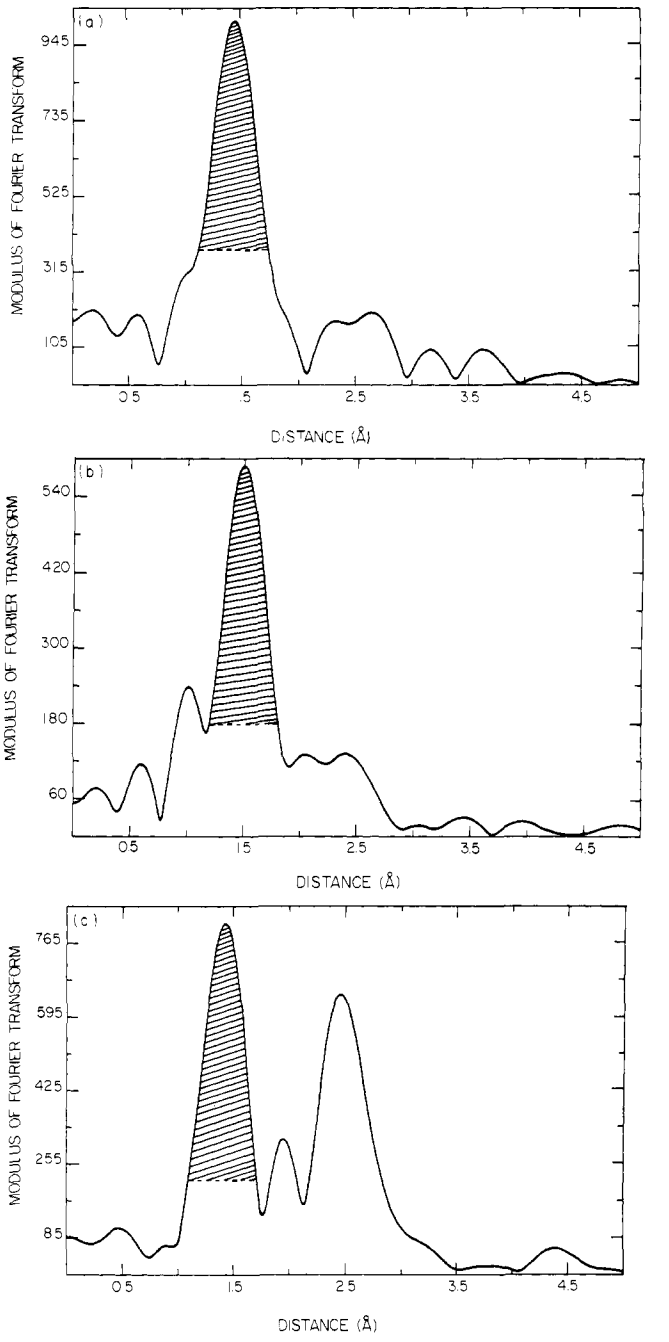

Figure 4. Modulus of the FT of the k^3 weighted EXAFS: (a) $Co(acac)_3$, (b) $[Co(en)_3Cl_3]$, (c) $K_3[Co(CN)_6]$. The shaded area in each transform represents the region of r space which was back-transformed into k space by using the windowing procedure described in the text.

where the subscript j denotes a new value and i the old one. Requiring that the phase remains unchanged implies that

$$\phi = \tan^{-1}\,[(\mathrm{Im})_i/(\mathrm{Re})_i] \tag{13}$$

and since

$$A_i = [(\mathrm{Re})_i^2 + (\mathrm{Im})_i^2]^{1/2}$$

and

$$A_j = [(\mathrm{Re})_j^2 + (\mathrm{Im})_j^2]^{1/2} \tag{14}$$

we solve for $(\mathrm{Re})_j$ and $(\mathrm{Im})_j$:

$$(\mathrm{Im})_j = (\tan\phi)[(A_j)^2 - (\mathrm{Im})_j^2]^{1/2}$$

$$(\mathrm{Im})_j = \pm\left[\frac{[(\tan^2\phi)(A_j)^2]^{1/2}}{\tan^2\phi + 1}\right] \tag{15}$$

$$(\mathrm{Re})_j = \pm\,[(A_j)^2 - (\mathrm{Im})_j^2]^{1/2} \tag{16}$$

The signs in eq 15 and 16 are chosen such that the original signs of the real and imaginary components of the phase remain unchanged.

It is evident that the amplitudes will be smaller when this window method is used. This is not a serious problem in our present goal of identifying atoms from their phases since the phases remain unchanged. Other window techniques also change the amplitudes (see Results and Discussion).

Results and Discussion

The isolated EXAFS patterns for the cobalt series of compounds $Co(acac)_3$, $[Co(en)_3]Cl_3$, and $K_3[Co(CN)_6]$ are shown in Figure 3. The modulus of the k^3 weighted FT of each of these compounds is presented in Figure 4. The shaded portion of the first-shell peak in each transform represents the region of r space which was back transformed into k space by using the procedure described in the previous section. The total phase was extracted from the first-shell EXAFS by using the method described by Lee et al.[12] and subsequentially fitted to a polynomial in k (eq 8). The

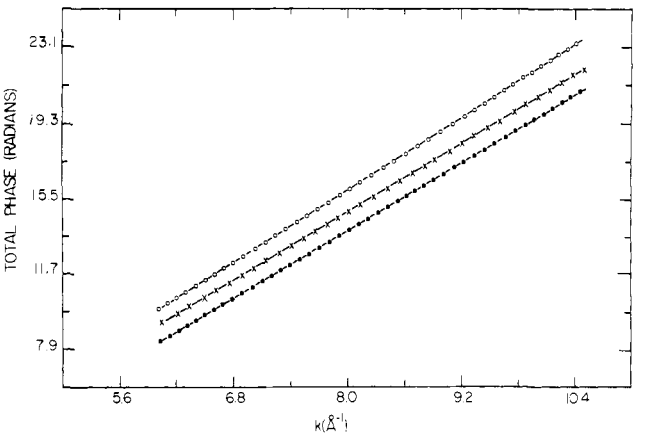

Figure 5. Total phase isolated from the first-shell peak in $Co(acac)_3$ (×), $[Co(en)_3]Cl_3$ (○), and $K_3[Co(CN)_6]$ (●). The solid curve represents the best fit to a quadratic function. Only every fourth data point is shown.

Table I. Coefficients from Least-Squares Fit to the Total Phase[a]

k range fitted, Å^{-1}	coeff	$Co(acac)_3$	$[Co(en)_3]Cl_3$	$K_3[Co(CN)_6]$
4.0–10.5	c_0	−7.746	−8.030	−8.517
	c_1	2.777	2.962	2.767
	c_2	0.0057	0.0041	0.0044
5.0–10.5	c_0	−7.722	−8.022	−8.475
	c_1	2.771	2.960	2.756
	c_2	0.0061	0.0043	0.0050
6.0–10.5	c_0	−7.682	−8.006	−8.412
	c_1	2.762	2.956	2.741
	c_2	0.0066	0.0045	0.0059
7.0–10.5	c_0	−7.634	−7.976	−8.320
	c_1	2.751	2.949	2.720
	c_2	0.0073	0.0049	0.0071
8.0–10.5	c_0	−7.692	−8.010	−8.393
	c_1	2.760	2.956	2.736
	c_2	0.0066	0.0045	0.0062

[a] Typical errors determined by the least-squares fitting program: c_0 ±0.004, c_1 ±0.001, c_2 ±5 × 10^{-5}.

fit was tried for several polynomials with different degrees in k. We have found that a second-order polynomial gives an adequate fit. Figure 5 shows the isolated phase together with the polynomial fit for each of the three compounds. Table I contains the coefficients of the polynomial fit for several fitted ranges of k space.

Table I shows that the constant coefficient in the polynomial fit for each of the three compounds is approximately independent of the fitted k range provided the minimum k value in the fit is greater than 6.5 Å^{-1}. This observation is in agreement with the calculated phases shown in Figure 1. Since only high k data are analyzed, the coefficients obtained from the fit are relatively insensitive to the choice of the threshold energy E_0. Furthermore, the small spread in the values of the coefficients in Table I may be attributed to a small higher order component in the phase. Note that the difference in the phase intercepts between the oxygen and carbon compounds is approximately 0.7 rad. This difference is smaller than that predicted by Figure 1 but is quite acceptable since the phases of oxygen and carbon converge somewhat at lower k values (Figure 1). Lee et al.[13] have shown that the composite phase shift function may be fitted to the function

$$\delta'(k) = c_0 + c_1k + c_2k^2 + c_3/k^3 \qquad (17)$$

and that the coefficients obtained are linear functions of atomic number over small regions of the periodic table. The quadratic form of eq 8 was used instead of that of eq 17 since the latter function is not defined at $k = 0$. Despite this, we have found that the phase intercept of the nitrogen compound lies approximately in between that of the oxygen and carbon compounds so that the constant coefficient is still an approximately linear function of atomic number (see Table I). This quadratic function, however, does not accurately describe the scattering phase for heavy atoms especially in the low k region.[13] Since EXAFS data from such heavy scatterers extend out to high k values, it is still possible to use the quadratic form of eq 8 provided only the high k data are fitted. This forms the basis for identification of scattering atoms which are heavier than those discussed here.

It should be noted, however, that the phase can only be calculated to within an arbitrary factor of π.[14] If 3π is added to the phase intercepts for the oxygen and carbon compounds, intercepts of 1.756 and 1.049 rad are obtained, respectively. These intercepts are in good agreement with the values calculated by Lee et al,[13] especially when the range of the fitted data is considered. A factor of $n\pi$ should, however, be easily identifiable since the separation between the phases of carbon and oxygen in Table I (see also Figure 1) is 0.7 rad, which is small in comparison to π. In practice, we have found that if the same data range is transformed for all compounds, there is no need to add or substract multiples of π.

The ability to distinguish between and identify different scattering atoms is dependent on the manner in which the EXAFS data are treated. The isolated phase extracted from experimental data is sensitive to windowing effects. In the forward transform no window function was used; the data analyzed began and ended at a node. This procedure yields good results provided an accurate background absorption has been determined and has been subtracted such that the end points chosen for the analysis are true nodal points.

The isolation of a peak in r space is more difficult, however, since the peak amplitude rarely drops rapidly to zero because of the nonlinearity in the phase, and the peak also usually contains side lobes due to termination errors in the transform. Any isolation procedure results in the data in the inverse space being the convolution of the FT of the isolated data with the FT of the window function. If a high-percentage Gaussian window is used, the FT of the isolated peak is convoluted with a narrow Gaussian in k space. In addition, the data in k space also contain much of the information which was present in the side lobes around the base of the peak. To eliminate this problem, a low-percentage Gaussian window may be used. However, the FT of the isolated peak is then convoluted with a wide Gaussian in k space. In principle, it is possible to remove the effects of the window function by deconvolution. In practice, however, this procedure introduces noise and suffers from the same problems as those found in the original transform.

As an alternative to the above methods we have introduced a new isolation procedure. As described in the previous section, the phase information is constrained to be the same as that in the original peak in r space while the amplitude is reduced such that the real and imaginary parts of the transform begin and end at a node. A comparison of this method with other isolation methods is shown in Figure 6. The data shown in this figure are from the isolated first-shell peak in $[Co(en)_3]Cl_3$. Note the distortions present in the amplitude and phase of the isolated peak when 20% (dotted curve) and 5% Gaussian windows (dashed curve) are used. As noted by previous investigators the distortion appears to be greatest in the first and last oscillations in k space.[12] This, however, does not guarantee that the data in between are undistorted since the sides of the peak which are multiplied by a Gaussian window function in r space receive a contribution to their intensity from all points in k space. The distortion is greatest in the first and last oscillation in k space because the amplitude of the original

(12) Lee, P. A.; Citrin, P. H.; Eisenberger, P.; Kincaid, B. M. *Rev. Mod. Phys.* **1981**, *53*, 769.
(13) Lee, P. A.; Teo, B. K.; Simons, A. L. *J. Am. Chem. Soc.* **1977**, *99*, 3856.
(14) Taylor, J. R. "Scattering Theory"; Wiley: New York, 1972; p 181.
(15) Stern, E. A.; Bunker, B.; Heald, S. M. "EXAFS Spectroscopy: Techniques and Applications"; Teo, B. K., Joy, D. C., Eds.; Plenum Press: New York, 1981; p 59.

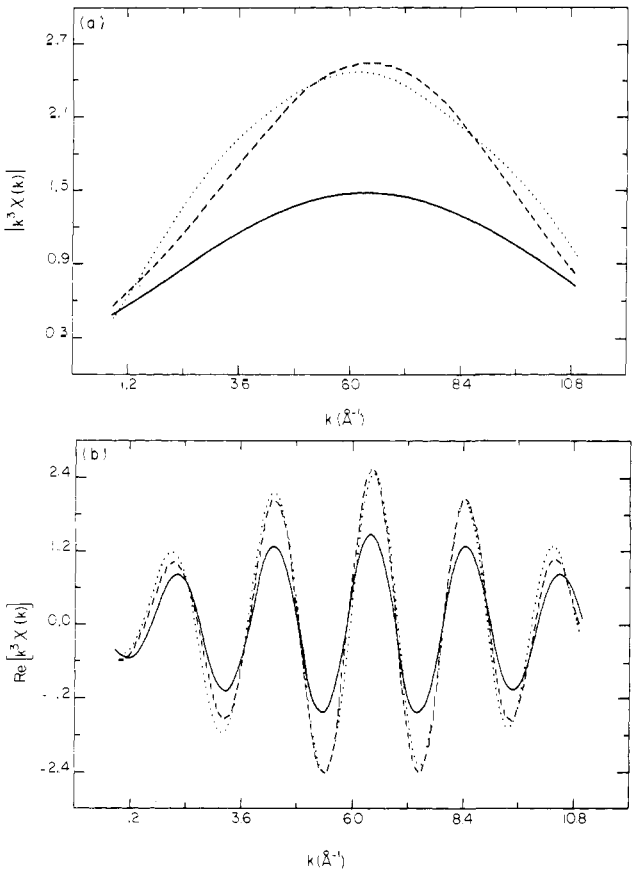

Figure 6. Comparison of the new windowing procedure with the earlier methods. The first-shell peak in the $[Co(en)_3]Cl_3$ compound was isolated by using the present method (solid curve) and 20% (dotted curve) and 5% Gaussian windows (dashed curve). (a) Modulus of the k^3 weighted EXAFS. (b) Real component of the k^3 weighted EXAFS.

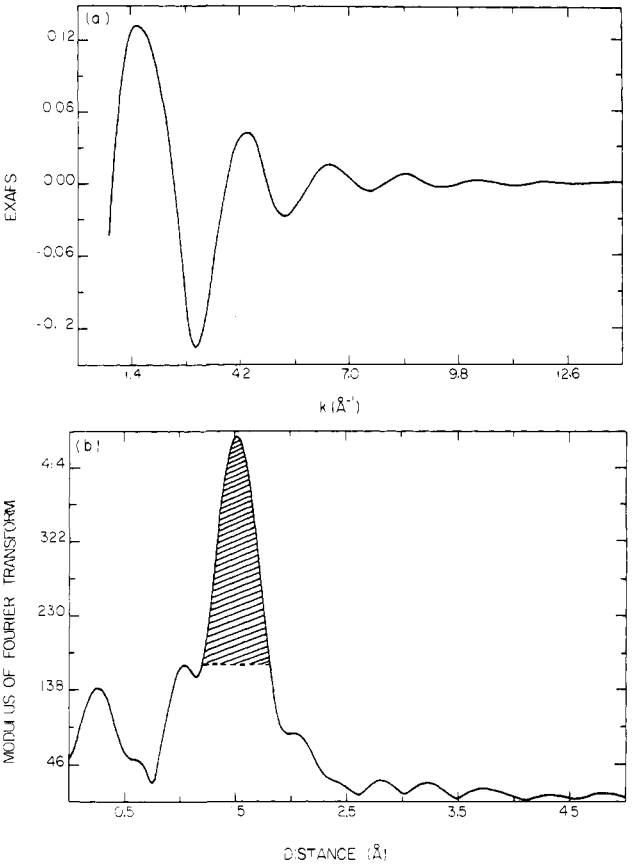

Figure 7. (a) Isolated EXAFS from $[Co(NH_3)_6]Cl_3$. (b) FT of the k^3 weighted EXAFS shown in part a.

data is smallest in these regions. The present method (solid curve) does not introduce such distortions since no window function has been employed. This method, however, does suffer from the usual termination effects due to the finite data range in the discrete transform.

We have found this new peak isolation technique to be superior when an accurate phase measurement is required. Since the atom-identification scheme requires an accurate knowledge of the phase intercept, slight distortions in the phase due to the usual windowing procedures are sufficient to make such a measurement impractical. The coefficients obtained from the quadratic fit are moderately sensitive to the width of the peak transformed in r space. This can be explained by considering the nature of the peak shape. Each peak in r space contains, due to phase nonlinearity, a distribution of frequencies from k space. The quadratic form used here may contain the most significant terms in such a distribution but not all of them. It is clear then that FT of peaks in r space with different widths may contain variable contributions of higher order terms in k. Accordingly, the most reliable phase intercepts are obtained when the peaks in r space are transformed with the same width (base of dashed area in Figure 4).

To illustrate the quantative nature of this atom identification scheme a fourth compound, $[Co(NH_3)_6]Cl_3$, was studied. The raw data, isolated EXAFS, and k^3 weighted FT of this compound are shown in Figure 7. When the procedure described above was used, the phase of the first-shell peak was extracted and fitted to a quadratic function. The coefficients of the fit are shown in Table II for a series of fitted k ranges. Note that the phase intercept for this compound is virtually identical with that obtained for $[Co(en)_3]Cl_3$ (see Table I). Therefore, if $[Co(NH_3)_6]Cl_3$ were an unknown compound, a comparison of its phase intercept with the three model compounds studied earlier would reveal that $[Co(en)_3]Cl_3$ is the appropriate model compound and that the scattering atom is a nitrogen.

Table II. Coefficients from Least-Squares Fit to the Total Phase of $[Co(NH_3)_6]Cl_3$[a]

k range fitted, Å^{-1}	c_0	c_1	c_2
4.0–10.5	−8.087	2.957	0.0058
5.0–10.5	−8.065	2.952	0.0054
6.0–10.5	−8.034	2.944	0.0058
7.0–10.5	−7.983	2.932	0.0065
8.0–10.5	−8.041	2.945	0.0058

[a] Typical errors determined by the least-squares fitting program: c_0 ±0.004, c_1 ±0.001, c_2 ±5 × 10^{-5}.

In many instances, however, the first coordination sphere is comprised of different types of atoms. If the separation in distance is greater than 0.4 Å the FT will distinguish between the different distances and the above analysis may be applied to each separate peak. Often this is not the case and only one first-shell peak is observed in the FT. When this happens the isolated phase is dependent upon the amplitude of the individual components which make up the peak. Consider a two-component first shell consisting of N_A atoms of type A and N_B atoms of type B. Clearly

$$N_A + N_B = N \tag{18}$$

where N is the coordination number of the first shell. Let $A(k)$ and $B(k)$ be the EXAFS amplitudes of components A and B, respectively. The EXAFS corresponding to the first-shell peak is given by

$$Z(k) = A(k) \sin \phi_A(k) + B(k) \sin \phi_B(k) \tag{19}$$

where $\phi_A(k)$ and $\phi_B(k)$ are the total phases of components A and B. If eq 19 is Fourier transformed and only the positive distances are retained, then the back-transformed EXAFS may be described by[12]

$$Z(k) = (1/2i)[A(k)e^{i\phi_A(k)} + B(k)e^{i\phi_B(k)}] = |\hat{Z}(k)|e^{i\theta(k)} \tag{20}$$

The observed amplitude is given by

$$Z(k) = \tfrac{1}{2}[A^2(k) + B^2(k) + 2A(k)B(k)\cos(\phi_A(k) - \phi_B(k))]^{1/2} \quad (21)$$

while the observed phase may be expressed as

$$\theta(k) = \tan^{-1}\left[\frac{A(k)\sin\phi_A(k) + B(k)\sin\phi_B(k)}{A(k)\cos\phi_A(k) + B(k)\cos\phi_B(k)}\right] - \frac{\pi}{2} \quad (22)$$

A factor of $\pi/2$ is typically added to eq 22 to yield the physically significant phase $\theta'(k)$.[12] If each of the phase functions can be parameterized as follows

$$\phi_A(k) = a_0 + a_1k + a_2k^2$$
$$\phi_B(k) = b_0 + b_1k + b_2k^2 \quad (23)$$

then the extrapolated value of the phase intercept is given by

$$\theta'(0) = \tan^{-1}\left[\frac{A(0)\sin a_0 + B(0)\sin b_0}{A(0)\cos a_0 + B(0)\cos b_0}\right] \quad (24)$$

If the total coordination number is known and we assume that

$$A(k)/B(k) \sim N_A/N_B \quad (25)$$

then the nature of the coordination sphere may be determined since we have two equations, eq 18 and 24, and two unknowns, N_A and N_B. When the phase intercepts shown in Table I were used, eq 24 was plotted in Figure 8 as a function of N_A and N_B assuming the approximation in eq 25 to be valid. For any observed phase intercept $\theta'(0)$ in Figure 8 there are two possible compositions of the first shell. In general, however, only one of these compositions will correspond to an integer number of atoms.

The approximation in eq 25 is unfortunately not generally valid. In the worst case of a coordination sphere made up of oxygen and carbon atoms the scattering amplitude of the oxygen can be approximately 30% greater than that of the carbon.[10] The metal–carbon bond distance, however, is typically shorter than the corresponding oxygen distance which partially offsets the difference in the scattering amplitudes. In general, eq 25 should be rewritten as

$$A(k)/B(k) = \left(\frac{N_A}{N_B}\right)X \quad (26)$$

where X is a factor, assumed to be constant, which represents the ratio between the EXAFS amplitudes of components A and B. Equation 26 must be substituted into eq 24 to obtain the true dependence of the phase intercept on the number of atoms in each component. If component A is oxygen and component B is carbon then Table III shows the observed phase intercepts for several X values. Note that increasing the value of X shifts the phase intercept to a more positive value and hence weights more strongly the contribution of the oxygen atoms to the observed phase. This shift, however, is small so that even if the EXAFS amplitude due to oxygen is 50% greater than that due to carbon the composition of the shell will still be distinguishable from other possible compositions (Table III).

It should be noted that for this method to yield reliable identification, several criteria must be met. The raw EXAFS data should be of high quality for both the unknown and model compounds. The subsequent analyses of the data should be performed in the same manner for all compounds. Incorrect estimation of E_0 presents a major problem. Our method of isolating E_0[11] should be adequate for compounds that do not differ greatly in their edge structure. If a known compound shows edge structures which differ from those of the unknown, this compound must be viewed as an unsuitable model for the unknown. The fact that the present method has yielded adequate identification of three different scatterers shows, however, that small deviations in E_0 (for E_0's isolated in the same way) do not present a great problem in the fitting. This is particularly true when only high k data are used to identify scatterers. It must be also noted that mixed-shell identification should be attempted only with data of very high signal-to-noise ratio.

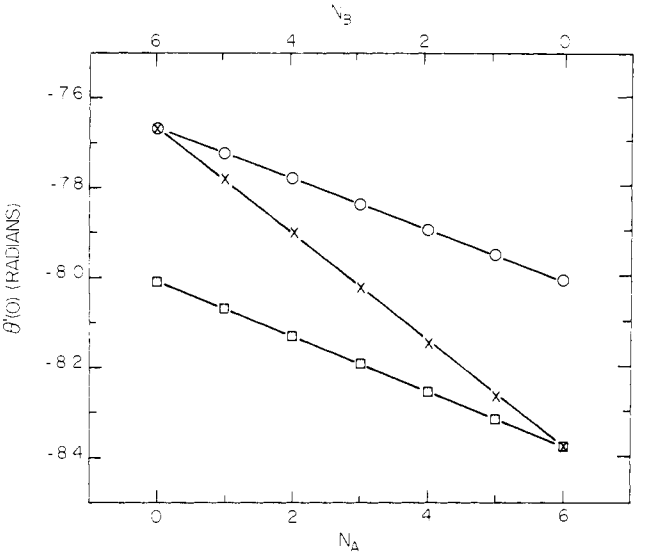

Figure 8. Phase intercept for a coordination shell of six atoms containing N_A and N_B atoms of types A and B. Component A always refers to the lighter of the two atoms. Nitrogen and oxygen (○); carbon and oxygen (×); carbon and nitrogen (□). The phase intercepts for the individual pure components were taken to be the average of the values shown in Table I. This figure was generated by using eq 24 and 25.

Table III. Calculated Phase Intercepts for a Two-Component System[a]

N_A	N_B	$\theta'(X = 1.0)$	$\theta'(X = 1.25)$	$\theta'(X = 1.5)$
0	6	−7.6690[b]	−7.6690	−7.6690
1	5	−7.7812	−7.7613	−7.7474
2	4	−7.8998	−7.8654	−7.8398
3	3	−8.0220	−7.9811	−7.9484
4	2	−8.1442	−8.1068	−8.0746
5	1	−8.2629	−8.2396	−8.2178
6	0	−8.3750[b]	−8.3750	−8.3750

[a] Component A is carbon and component B is oxygen. [b] Phases for the pure components are the average of those values shown in Table I.

The identification scheme introduced here represents a contribution to current EXAFS data analyses methods. The examples shown demonstrate the distinguishability of carbon, nitrogen, and oxygen in a series of cobalt complexes. These three atoms represent important scatterers, the identification of which may help to resolve significant structural problems. For example, in metalloproteins, the first-shell metal ligands consist primarily of nitrogen, oxygen, and sulfur from the protein amino acids. Since this approach can be readily extended to other scattering atoms, there should be numerous chemical applications of this identification scheme.

Registry No. $Co(acac)_3$, 21679-46-9; $[Co(en)_3]Cl_3$, 13408-73-6; $K_3[Co(CN)_6]$, 13963-58-1; $[Co(NH_3)_6]Cl_3$, 10534-89-1.